Hindawi
Advances in Civil Engineering
Volume 2023, Article ID 7297089, 15 pages
https://doi.org/10.1155/2023/7297089

Review Article

Multiple Disturbances of Existing Tunnels Caused by Deep Excavation and New Shield Tunnel

Haoran Li, Fei Ye, Enjie Su, and Xingbo Han

School of Highway, Chang'an University, Xi'an, Shaanxi 710064, China

Correspondence should be addressed to Haoran Li; 2019021072@chd.edu.cn

Received 8 May 2023; Revised 3 June 2023; Accepted 28 October 2023; Published 24 November 2023

Academic Editor: Junwei Ma

With the continuous development of urban underground spaces, new underground engineering approaches are becoming more similar to existing operating tunnels. Existing research is typically concerned with the impact of a single project, such as a new tunnel or deep excavation, on existing shield tunnels. There are few studies on the influence of both excavation and overcrossing tunneling on operational tunnels. Taking a section ranging from the Chengzhan Station to the Jiangcheng Road Station of Hangzhou Metro Line 7 as a case study, this study analyzes the automatic monitoring data of the existing tunnel within this section. Through data analysis, the influences of deep excavation and shield tunneling on the vertical settlement, horizontal displacement, segment convergence, and differential settlement of the tunnel ballast of the adjacent existing line segment are assessed. The influence of deep excavation and overcrossing tunneling on multiple disturbances of existing line tunnels is summarized. This study will be useful for similar projects involving deep excavation next to existing tunnels and overcrossing tunneling, as it will help clarify the protection range of existing lines and determine the displacement alarm value of existing structures.

1. Introduction

With the rapid development of urban rail transit in China, the density of subway line networks has gradually increased [1]. All kinds of deep excavations are inevitably adjacent to the rail transit structure, and it is unavoidable that new tunnels and existing tunnels overlap with each other when the construction of new projects or the reconstruction of old projects is implemented [2]. Owing to its fast construction speed, high safety performance, small environmental interference, and small surface deformation, the use of a shield has become the main method of underground space development in densely populated and congested cities. Therefore, the scope of the discussion in this study is limited to existing and new tunnels constructed using a shield. The tunnel structure comprises prefabricated segments assembled by bolts, which endow it with many joints, weak integrity, and low overall stiffness. The stress change and soil deformation caused by construction activities near the operation line are likely to have adverse effects on the subway structure. In terms of engineering, many studies have shown that improper construction leads to excessive displacement, deformation, segment damage, and even engineering accidents in adjacent subway tunnels [3–7]. Some scholars have also proposed quantitative analysis and evaluation approaches for possible damage to existing tunnels [8]. Therefore, it is critical to investigate the deformation and displacement of existing tunnels [9].

Several studies have been conducted on the construction of deep excavations near existing lines. The main research methods include numerical simulation [10–13], analysis of measured data [14–16], theoretical calculation [17–19], and model test [20–22]. Zhang et al. [15] investigated the deformation of adjacent subway segments caused by different block parameters during deep excavations at the side and directly above the tunnel. Huang et al. [8] investigated the change characteristics of the additional bending moment and deformation of a tunnel at different buried depths under deep excavation through a centrifugal model test. The results show that the influence of the deep excavation on the tunnel is within 2.5 times the excavation width from the boundary of the deep excavation and the vertical deformation of the

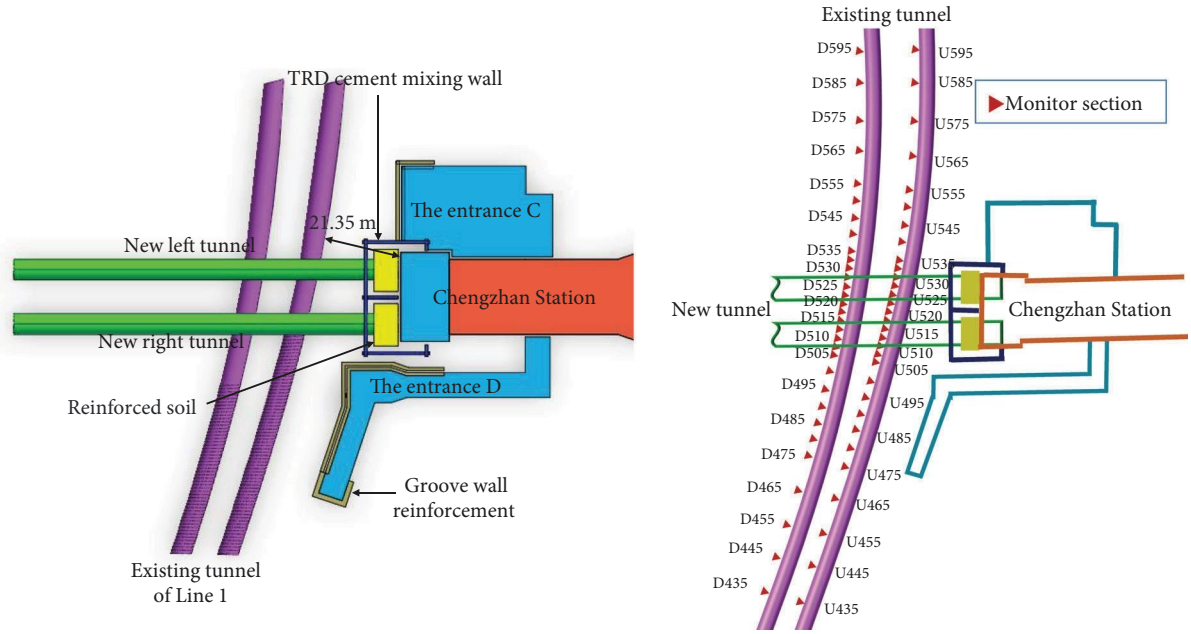

Figure 1: Plan view layout of the project.

tunnel decreases exponentially with an increase in the distance between the pit bottom and the tunnel. When this distance is greater than 1.5 times the excavation depth, the additional bending moment generated by excavation unloading on the tunnel section can be ignored [20]. Nie et al. [23] analyzed the influence of excavation unloading on the vertical and horizontal displacement of existing tunnel segments under the side using FLAC 3D. Gao et al. [24] analyzed the development law of the overall displacement of a tunnel and the deformation of the tunnel structure during excavation and structural load construction in different areas on the side and above the tunnel. Wei et al. [25] hypothesized that changes in the confining pressure of the side tunnel cross-section are caused by deep excavations.

Currently, there are mainly studies on the impact of shield tunneling on existing tunnels based on various methods, such as the empirical formula method [26, 27], theoretical research method [28–30], simulation experiment method [31, 32], field measurement method [12, 33, 34], and numerical simulation method [35–37]. Li [38] regarded an existing subway tunnel as an Euler–Bernoulli beam model placed on a Riftin foundation model. On the basis of the "two-stage analysis method," Li [38] proposed a calculation method for the uplift displacement of the existing tunnel caused by the new tunnel overcrossing project. Chen et al. [32] used Shanghai Metro Line 8 short-distance overcrossing subway Line 2 as the research background and analyzed the variation characteristics of longitudinal settlement of the large-angle overcrossing existing tunnel in the short distance according to field monitoring data. Ding et al. [39] concluded that the influence of shield crossing on an existing tunnel is mainly due to uplift deformation and that the deformation curve is parabolic based on field measurement data. Yang et al. [40] analyzed the influence of a shield on an existing tunnel and stratum in the shield tunneling process under different stratum loss rates through numerical simulations.

However, currently, there are few studies on the effects of both excavation unloading and overcrossing disturbances of new tunnels on existing lines, and similar engineering cases are uncommon. The displacement, deformation, and internal force of an existing tunnel subjected to multiple disturbances are more complicated than those of an existing tunnel subjected to a single disturbance. Therefore, it is necessary to investigate the displacement and deformation of an existing tunnel structure under multiple disturbances.

An existing tunnel, adjacent to a deep excavation excavated at a final depth of 16.67 m in the downtown area of Hangzhou and straddled by a new shield tunnel, was extensively instrumented. Subsequently, the site conditions, geology, instrumentation, and construction sequence were first reported. Then, the vertical and horizontal displacement and convergence of the tunnel segment and differential settlement of the ballast bed, induced by excavation, were analyzed. Finally, the above features were analyzed again for shield tunneling.

2. Project Description

The underground line adopted was the SG7-2 section of Hangzhou Metro Line 7 engineering civil construction from the Chengzhan Station to the Jiangcheng Road Station. The shield tunneling machine begins from the Chengzhan Station to the Jiangcheng Road Station. The Chengzhan Station is designed as an underground two-storey island station. Figure 1 shows the excavation depth of the shield initiation well at the Chengzhan Station is 16.7 m, and the depth of the diaphragm wall is 33.3 m. Because the shield initiation well is close to an existing tunnel (the nearest place is only 21.35 m),

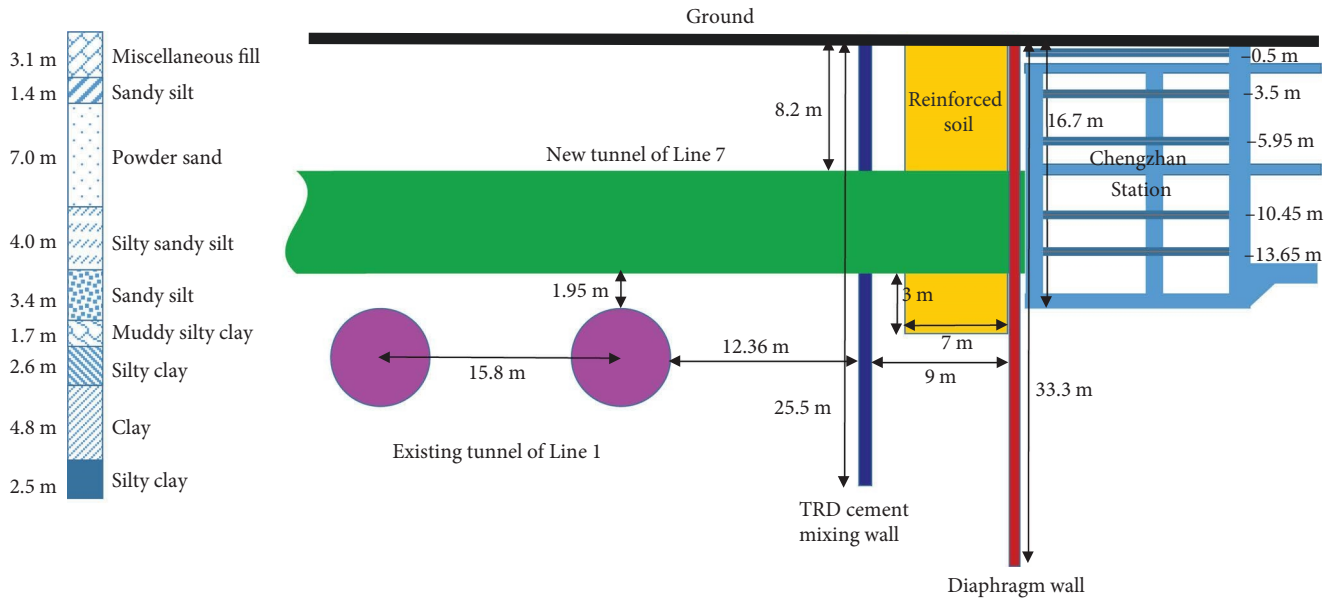

Figure 2: Layout diagram of the new pit and tunnel and the existing tunnel.

to prevent excessive disturbance to the existing line caused by the deep excavation, a diaphragm wall of isolation is added between the shield initiation well and the standard section. The separation wall will be broken during the construction of the main structure. The retaining structure of the main foundation pit of the Chengzhan Station adopts an 800-mm-thick diaphragm wall at a depth of 33.04 m. The length, width, and depth measurements of the shield initiation well excavation are 25.8, 18.1, and 16.67 m, respectively. Figure 2 shows soil excavation is performed in five steps to levels of −4, −6.45, −10.95, −14.15, and −16.67 m. Consequently, two layers of concrete struts are designed at the levels of −0.5 and −5.95 m, and three layers of steel struts are designed at the levels of −3.5, −10.45, and −13.65 m, with a thickness of 16 mm and an outer diameter of 800 mm. The width and height of the first layer of concrete struts are 1,000 and 800 mm, respectively. The width and height of the second layer of concrete struts are 800 and 1,000 mm, respectively. The main structure of the shield initiation well comprises the bottom, middle, and top plates. The material is C35 reinforced concrete, and the thicknesses are 1,000, 400, and 800 mm, respectively, at depths of −11.67, −7.48, and −2.04 m, respectively. In addition, the top and bottom concrete materials have waterproof requirements.

The distance between the entrance and exit of C and the nearest place of the existing tunnel is ∼21 m, and the depth of the foundation pit is 8.2–11.2 m. The diaphragm wall is 600 mm thick, and the depth of the standard section is 22.5 m. Soil excavation is performed in three steps to levels of −3.9, −6, and −8.25 m. Consequently, one layer of concrete struts is designed at a level of −0.4 m with 800 mm width and 800 mm height, and two layers of steel struts are designed at levels of −3.4 and −5.5 m, with a thickness of 16 mm and an outer diameter of 609 mm. The structure consists of a bottom plate and a top plate. The material is C35 reinforced concrete. The top plate is 600 mm thick, the bottom plate is 700 mm thick, and the top and bottom concrete materials have waterproof requirements.

The distance between the entrance and exit of D and the nearest place of the existing tunnel is ∼13 m. The excavation depth of the foundation pit is 9.09–12.09 m. An underground diaphragm wall of 600 mm thickness is adopted in the enclosure structure, and the underground diaphragm wall of the standard section is 23.2 m. Soil excavation is performed in three steps to levels of −3.4, −6.5, and −8.25 m. Consequently, one layer of concrete struts is designed at a level of −0.4 m with 800 mm width and 800 mm height, and two layers of steel struts are designed at levels of −2.9 and −6 m, with a thickness of 16 mm and an outer diameter of 609 mm. The structure consists of a bottom plate and a top plate. The material is C35 reinforced concrete. The top plate is 600 mm thick, the bottom plate is 700 mm thick, and the top and bottom concrete materials have waterproof requirements.

Because both the initiation and reception of shield tunneling are high-risk working conditions, it is typically necessary to adopt a triaxial mixing pile for reinforcement within 9 m of the shield initiation well. In this case, to prevent excessive disturbance to the existing operating tunnel, the starting section was strengthened using a TRD cement mixing wall, and the interior was strengthened using a triaxial deep cement mixing pile, as shown in Figure 1.

The soil should have good uniformity, independence, and water retention, and its unconfined compressive strength should not be less than 1 MPa after reinforcement. The thickness of the cement mixing wall is 850 mm, and the depth is 25.5 m, which is 3 m lower than the bottom of the existing tunnel. The three-axis mixing pile is reinforced with a diameter of 850 mm and a spacing of 600 mm and is constructed according to the nesting and one-hole method. The reinforcement depth of the three-axis mixing pile is 17.4 m, which is 3 m lower than the bottom of the new tunnel. At the sides of

Table 1: Physical and mechanical parameters of soil.

Strata sequence	Soil	Natural unit weight, γ (kN/m^3)	Cohesion, c (kPa)	Angle of friction, φ (°)	Soil thickness (m)
1-1	Miscellaneous fill	17.5	8	15	3.1
3-2	Sandy silt	19.5	6	29	1.4
3-3	Powder sand	19.3	5	33	7.0
3-5	Silty sandy silt	19.2	5	33	4.0
3-7	Sandy silt	19.6	6	28	3.4
6-2	Muddy silty clay	19.2	25	15	1.7
7-2	Silty clay	19.1	28	18	2.6
8-1	Clay	19	25	19	4.8
8-2	Silty clay	18.8	20	20	2.5

the C and D entrances close to the existing line, groove wall reinforcement is set at the diaphragm wall. The reinforcement process also adopts the reinforcement process of the triaxial cement mixing pile. The reinforcement depth is the same as the depth of the diaphragm wall. In addition, in this case, dewatering wells are established inside and outside the foundation pit. However, because the dewatering wells inside and outside the pit are within the range of concrete sealing, they have little influence on the existing tunnel. The influence of groundwater dewatering is not considered in this study.

The distance between the upline and downline tunnels of the shield section from the Chengcheng Station to the Jiangcheng Road Station is ∼14.6–16.2 m, and the buried depth of the tunnels is 8.3–20.6 m. The Chengzhan Station is adjacent to the section tunnel of Metro Line 1, which is operational. The proposed tunnel will cross Line 1, which is already operational, at an oblique angle of 80°. The minimum vertical distance between the two tunnels is 1.95 m.

Both the new and existing tunnels are excavated using earth pressure balance shield machines. Concrete segments are assembled with staggered joints. The inner and outer diameters of the tunnel are 5,500 and 6,200 mm, respectively. The thickness of the segments is 350 mm, and the width of the prefabricated reinforced concrete segments is 1,200 mm. The strength grade of the segment is C50, which is divided into six pieces in the circumferential direction. Figure 2 shows the buried depth of the existing tunnel of Line 1 is ∼16.4 m, and the spacing between the left and right lines is ∼16.0 m. The buried depth across the existing tunnel section of the new tunnel is ∼8.2 m. The distance between the left and right lines is ∼15.8 m.

3. Geology and Soil Parameters

According to the geotechnical investigation report of Hangzhou Metro Line 7, the basic and model parameters of soil mass are obtained by combining the results of the indoor soil test, in situ test, and hydrogeological test.

Table 1 shows that the topsoil layer is a miscellaneous fill (layer 1) with a thickness of 3.1 m, which is underlain by sandy silt (layer 2) with a thickness of 1.4 m. The third layer is a 7-m-thick layer of powder sand (layer 3) containing iron oxide spots and mica debris, with a thin layer of clay. The following layer is silty sandy silt (layer 4) with a thickness of 4 m, which is saturated, medium dense, and locally slightly dense. It contains mica debris with a small amount of clay clump locally. The next layer is a 3.4-m-thick layer of sandy silt (layer 5) consisting of mica debris. Below this layer is a 1.7-m-thick layer of muddy silty clay mixed with silt (layer 6). The seventh layer is a 2.6-m-thick silty clay layer (layer 7), and plastic, local hard plastic, and dry shrinkage cracks can be observed after water loss. The next layer is a 4.8-m clay layer (layer 8), mainly composed of soft plastic and local fluid plastic containing organic matter. The final layer is a 2.5-m-thick silty clay layer (layer 9). It is soft plastic, local fluid plastic with a silt content of ∼10%–30%, viscoplastic, and contains mica debris.

From the soil weight analysis, the soil weight of the hybrid fill is small (17.5 kN/m^3), whereas the soil weight of other soil layers is between 18.8 and 19.6 kN/m^3, which is large, mainly because of the existence of groundwater. Soil 2 m below the surface is saturated. The cohesiveness of the soil in the first five layers is less than 10 kPa, whereas the cohesiveness of the soil in the subsequent layers is between 20 and 25 kPa. This is mainly because, with the change of strata, the nature of the soil gradually changes from sandy to cohesive, resulting in a sharp increase in cohesion. The internal friction angle of the second to fifth layers is large, ranging from 28° to 33°, whereas that of the remaining layers, including the hybrid layer, is not larger than 20°, which is mainly caused by the difference between sandy and cohesive soil, as shown in Table 1.

4. Automatic Monitoring Arrangement and Monitoring Content

The automatic monitoring method was used to monitor the existing tunnel immediately after the soil reinforcement construction began. The existing tunnel was continuously monitored throughout the construction cycle, including the construction of the envelope structure, excavation of the foundation pit, and the overcrossing period of the new shield.

The automatic monitoring system mainly comprises a small prism, rearview control prism, total station, transmission module, and client. As monitoring points, small prisms are buried in tunnels or stations. The rearview control prism is used as a reference point, and the borehole is buried in a

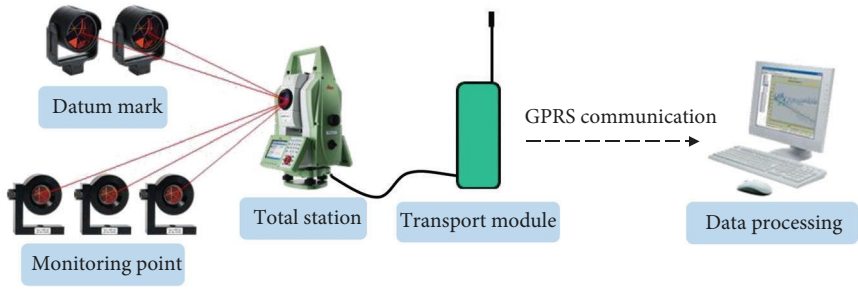

Figure 3: Automatic monitoring system.

stable position. The total station adopts a fixed instrument table for 24-hr automatic measurements and is supplemented by manual retesting. The transmission module is used for real-time data transmission and control. Real-time control and data processing using a computer are achieved by the user. This project adopts the TM50 total station produced by Leica of Switzerland, which has the highest accuracy in the world at present. The angle measuring accuracy is "0.5," and the ranging accuracy is 0.6 mm + 1 ppm. With ATR automatic aligning technology, a new spot analysis method is used to optimize the prism verification method. It can automatically learn target prisms at ultra-long distances, automatically identify effective prisms with one key, eliminate interference factors in the environment (light, moisture, sunshine, etc.) and invalid targets, and effectively improve the distance, accuracy, and efficiency of automatic measurements.

Automated monitoring is performed using the Leica GeoMoS software, which consists of two main parts: a monitor and an analyzer. The monitor has a mature measurement and calculation program that provides an ideal solution for applications requiring extremely high accuracy. Profilers can graph and digitally present data, as illustrated in Figure 3.

According to the characteristics and relevant requirements of the project, automatic monitoring systems are established in the track running areas of the upline and downline, with monitoring lengths of ~200 m, respectively. Considering the accuracy of automatic measurements of the total station, monitoring alarm value, and site conditions, two total stations each are established in the upline and downline tunnels, totaling four total stations, and two automatic monitoring networks are constructed.

The monitoring facilities are set up as follows:

(1) The total station and rearview prism extend along the tunnel to reduce the plane displacement error caused by distance measurements.

(2) On both sides of the measuring area outside the influence range of the foundation pit, large rearview prisms are set up as control points, and at least four large prisms are set up at the large and small mileage ends.

(3) Each monitoring section is provided with four small prisms, which are located near the two steel rails of the ballast bed and on both sides of the lining segment as monitoring points.

(4) The automatic monitoring network is arranged as a 3D network, and the plane coordinates and elevation values are simultaneously measured.

Automatic monitoring is employed during the upper span of the shield tunnel. A monitoring section is set at 1–15 m outside the projection range of the shield tunnel at 2–3-ring intervals. A monitoring section is set at 15–55 m outside the projection range of the shield tunnel at 5-ring intervals. Two sets of monitoring prisms are set on both sides of the lining segment and the ballast bed. The vertical and horizontal displacements of the tunnel segments, the convergence of the segments, and the differential settlement of the ballast bed are monitored. The upline and downline monitoring ranges have 31 sections each. The monitoring range of the upper and lower line segments of the existing tunnel is 435–595 rings, as shown in Figure 1.

The monitoring content is the vertical displacement of the ballast bed, i.e., the average of the vertical displacements of prisms 1 and 2. A positive sign indicates uplift, and a negative sign indicates settlement. The horizontal displacement of the ballast bed is the average of the horizontal displacements of prisms 1 and 2. A positive sign indicates movement toward the foundation pit, whereas a negative sign indicates movement away from the foundation pit. Segment convergence is the distance between prisms 3 and 4. An increase in the distance indicates a positive value, and a decrease indicates a negative value. Similarly, the differential settlement of the ballast bed is the difference between prisms 1 and 2. An increase in the distance indicates a positive value, and a decrease indicates a negative value.

During the construction process, the survey team conducted 24 joint measurements of the datum point and manually reviewed the automatic monitoring data 84 times. The results showed that the maximum difference between the automatic and manual monitoring results of the upline and downline was ±2.1 mm, which is small and meets the requirements. Furthermore, the automatic monitoring data were authentic and credible. The monitoring arrangement is shown in Figure 4.

5. Construction Process

The construction factors affecting the existing tunnel are divided into five aspects: (1) soil reinforcement of the starting section and construction of the underground diaphragm

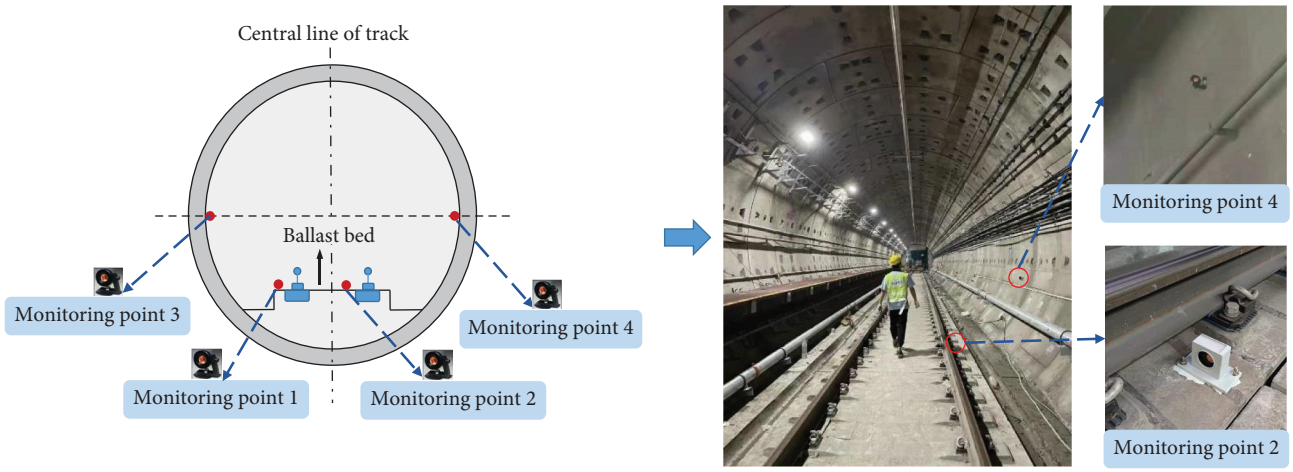

Figure 4: Layout of automated monitoring points on the segment.

wall; (2) foundation pit excavation and structure construction of the shield initiation well of the Chengzhan Station; (3) upper span of the left line shield of the new tunnel; (4) upper span of the right line shield of the new tunnel; and (5) excavation and structure construction of the foundation pit of the attached entrance and exit. Note that, due to land planning, only groove wall reinforcement was performed at entrance D, and the subsequent construction of an underground diaphragm wall, foundation pit excavation, and structural works were canceled. The specific construction process is detailed in Table 2.

6. Analysis of Monitoring Data of Existing Tunnels

Here, the main foundation pit of the station was excavated, and the left and right lines of the shield of the new tunnel were driven twice. The deep excavation of the entrance and exit of C repeatedly affected the existing tunnel. In this study, the displacement and deformation of the existing line tunnel are analyzed from four perspectives: vertical displacement, horizontal displacement, segment convergence, and differential settlement of the ballast bed.

6.1. Analysis of the Entire Process Data Change Law of Monitoring Points

6.1.1. Vertical Displacement. It can be observed from Figure 5(a) that the existing tunnel is slightly disturbed at the stage of soil reinforcement of the starting section, foundation pit excavation, and construction of the station main structure, and each segment has a small settlement, with the 528-ring settlement being the largest, with a value of 1.45 mm. This measurement result is consistent with those of Zheng et al. [41] and Meng et al. [42]. At the stage where the right line shield crosses the existing line tunnel, which is affected by soil unloading, the 435–518-ring segment uplifts, and the maximum value of the 508-ring uplift is 2.85 mm compared with the previous stage, as shown in Figure 6. However, the 525–535 rings still have slight settlement, mainly because the existing tunnel segment is a longitudinal integral structure. When a section is uplifted to a significant extent, there is slight settlement in the adjacent section. At the stage where the left line shield crosses the existing line tunnel, the 515–545 rings exhibit an obvious uplift trend and the 475–513 rings have a slight settlement compared with the previous stage. These measurement results are consistent with those of Chen et al. [4] in the uplift trend of segments but are slightly different in the settling part of existing lines [32]. The theoretical conclusion of Liang et al. [43] can better explain this phenomenon, as illustrated in Figure 6. During the foundation pit excavation of the entrance and exit of C, the 545–595 rings of its influence area have an obvious settlement, and the maximum value appears at the 575 ring with a settlement of 2.85 mm. The remaining points are consistent with the vertical displacement in the previous stage.

Figure 5(b) also shows at the stage of soil reinforcement of the starting section and foundation pit excavation of the main station, the existing tunnel segments are slightly affected within the range of 1 mm. At the stage of construction of the main structure of the station, 485–528 rings exhibit a settlement trend, and the maximum value appears at the 510 ring with a settlement of 1.40 mm. At the stage of right line shield construction across the existing tunnel, which is affected by soil unloading, the annular lining segments of the existing tunnel 485–520 rings appear to be uplifted. However, compared with the initial value, the uplift is not obvious, and the vertical displacement of other segments is consistent with that of the previous stage. At the stage where the left shield crosses the existing line, the settlement trend of 533–595 rings is obvious, while the settlement of 475–500 rings is drastic, and the settlement value of the 480 ring reaches 3.55 mm. This measurement result is highly consistent with that of Chen et al. [4] in terms of the variation trend and degree of vertical displacement of existing tunnel segments [31]. Compared with the previous stage, the existing tunnel is less affected during the foundation pit excavation of the entrance and exit of C, and there is no change compared with the previous stage.

6.1.2. Horizontal Displacement. In Figure 7(a), it can be interpreted that at the stage of soil reinforcement of the starting

Table 2: Construction process and schedule node.

Stage	Construction activity	Date	Remark
S1: soil reinforcement and enclosure structure	TRD cement mixing wall	2018.8.21–2018.9.3	The soil reinforcement and construction of the enclosure structure have less disturbance to the existing line
	Soil reinforcement of the triaxial mixing pile in the starting section of the shield	2018.8.20–2018.9.3	
	Construction of the diaphragm wall of the shield initial well	2018.10.30–2018.12.30	
	Groove wall reinforcement at the entrance and exit of D	2018.12.25–2019.1.3	
	Groove wall reinforcement at the entrance and exit of C	2019.1.4–2019.1.6	
	Construction of a diaphragm wall at the entrance and exit of C	2019.4.14–2019.4.27	
S2: foundation pit excavation and structure construction of the shield initial well	Foundation pit excavation and support erection	2019.5.25–2019.7.24	There is a significant disturbance to the existing line
	Main structure construction	2019.7.25–2019.10.31	The structure has been stabilized and the disturbance to the existing line is less
S3: the new tunnel crosses over the existing tunnel	New tunnel right line tunneling	2020.7.14–2020.8.23	The shield drove 100 rings, exceeding the influence range of the existing line
S4: the new tunnel crosses over the existing tunnel	New tunnel left line tunneling	2021.1.6–2021.1.22	
S5: excavation and structural construction of the pit at the entrance and exit of C	Foundation pit excavation and support erection	2021.3.3–2021.4.7	There is a great disturbance to the existing line
	Main structure construction	2021.4.8–2021.5.30	The structure has been stabilized and the disturbance to the existing line is less

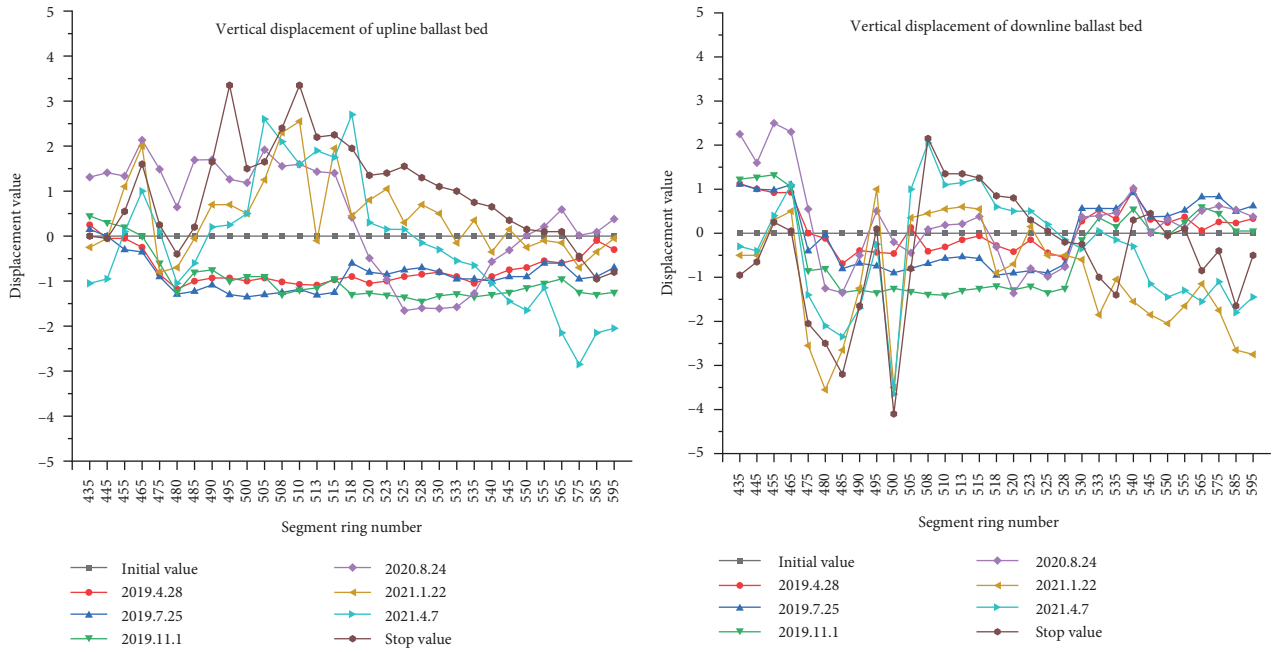

Figure 5: (a, b) Vertical displacement of existing tunnels under multiple disturbances.

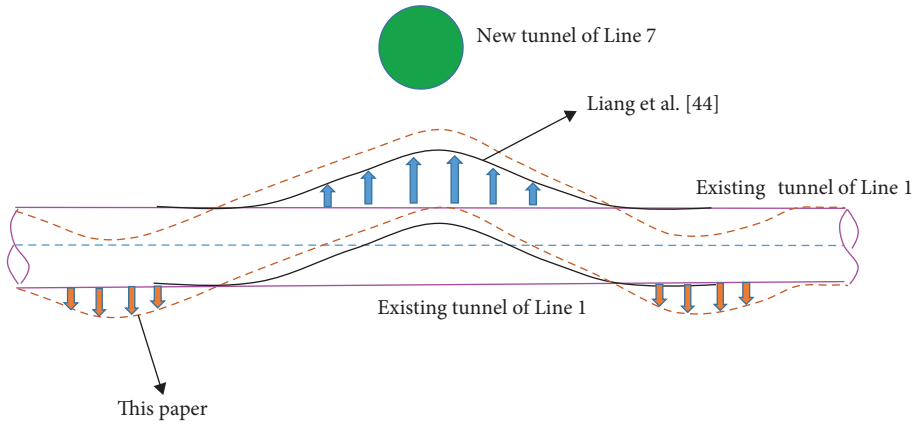

Figure 6: Slightly differences from previous studies on vertical displacement.

section, the horizontal displacement of the existing tunnel is slightly affected. At the stage of foundation pit excavation of the station, the segments of the existing tunnel significantly move toward the foundation pit, which is reflected in the range of 490–545 rings, with a maximum value at the 530 ring and a displacement value of 1.85 mm. At the stage of main structure construction, the existing tunnel is consistent with the previous stage without significant horizontal displacement. Similar to vertical displacement, this measurement result is consistent with the research conclusions of Yang et al. [40], Zheng et al. [41], and Meng et al. [42]. At the stage where the right line shield crosses the existing line tunnel, the 500–545 rings exhibit significant displacement away from the foundation pit, with a maximum value at the 528 ring and a displacement value of 3.80 mm. This is mainly because when the shield tunneling machine is driving, the shield shell exerts a dragging force on the soil in the tunneling direction, resulting in the surrounding soil and structure moving toward the shield tunneling machine. Compared with the previous stage, the segment of the existing tunnel did not experience significant disturbance in the horizontal direction. This is because the surrounding soil was strengthened by the synchronous and secondary grouting of the new tunnel segment, which reduced the influence of the shield tunneling machine. During the excavation of the entrance and exit of C, the 520–555 rings of the segment exhibit a displacement toward the foundation pit, and the horizontal displacement is ~2 mm compared with the previous stage. Finally, the horizontal direction of the existing tunnel segments did not change significantly, and the stop

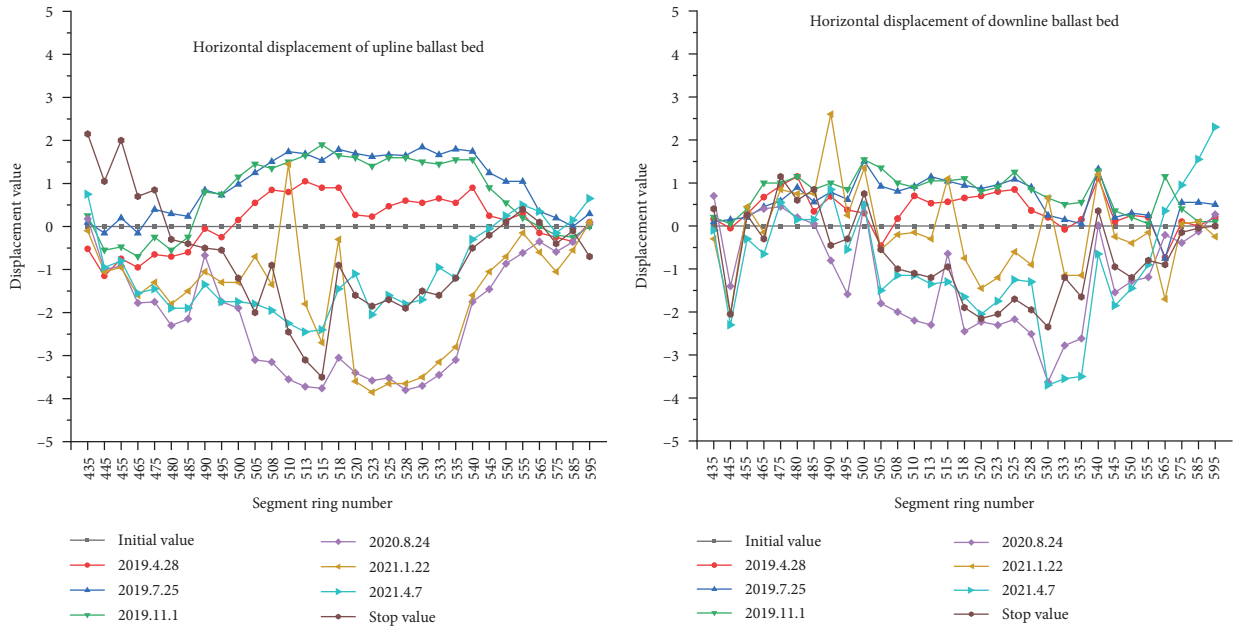

Figure 7: (a, b) Horizontal displacement of the existing tunnel under multiple disturbances.

value data were consistent with the data after the deep excavation of the entrance and exit of C.

Figure 7(b) shows that at the stage of soil reinforcement of the starting section, deep excavation, and main structure construction of the station, the downline segments of the existing tunnel move slightly toward the foundation pit with a maximum value at the 500 ring and a displacement value of 1.54 mm. At the stage where the right shield crosses the existing line tunnel, the horizontal displacement of the 490–585 rings is opposite to that in the previous stage and moves away from the foundation pit, as illustrated in Figure 8. The maximum displacement value appears at the 570 ring, which is 3.7 mm and is due to the drag force exerted by the shield machine on the soil. The horizontal displacement of the segments 505–555 rings sharply falls and oscillates around the initial value at the stage where the left shield crosses the existing line. At the excavation stage of the entrance and exit of C, the segments of the existing tunnel are not significantly affected, which is the same trend as in the previous stage, except that the 565–595 rings in the influence range of the entrance and exit of C move toward the foundation pit. The maximum value appears at the 595 ring, and the displacement is 2.3 mm.

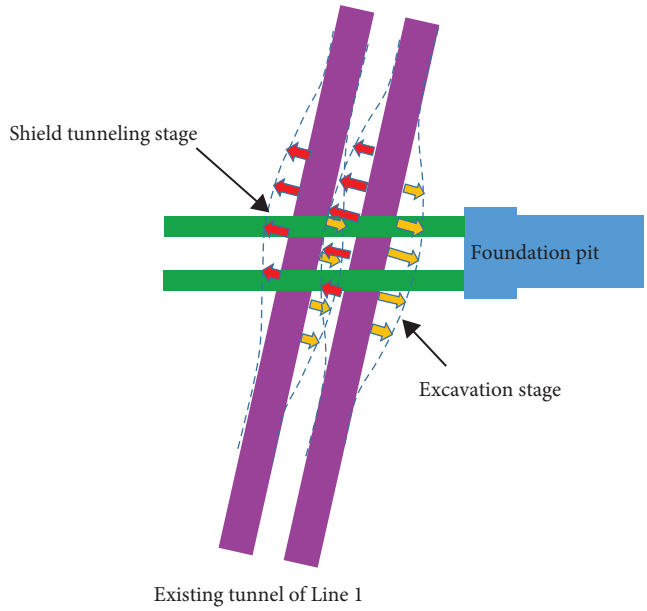

Figure 8: Horizontal displacement trend of the existing tunnel under multiple disturbances.

6.1.3. Segment Convergence. From inspection of Figure 9(a), the soil reinforcement of the starting section does not have a significant effect on segment convergence. At the stage of foundation pit excavation, the 508–545-ring segments of the upline of the existing tunnel produce vertical compression and transverse tension. The maximum tensile value is at the 523 ring, and the convergence value is 1.9 mm. At the stage of station structure construction, the existing tunnel is unaffected and the convergence value is consistent with that in the previous stage. At the stage of right and left line shield tunneling across the existing line, the convergence value of segments slightly decreases in the range of 500–535 rings and slightly increases in the range of 540–555 rings. The maximum value appears at the 545 and 555 rings, and the convergence value is 2.4 mm. However, the existing tunnel remains in a state of vertical compression and transverse tension. At the excavation stage of the entrance and exit of C, the convergence value of the existing tunnel segments is the same as that in the previous stage, and only a significant oscillation occurs in the range of 505–515 rings.

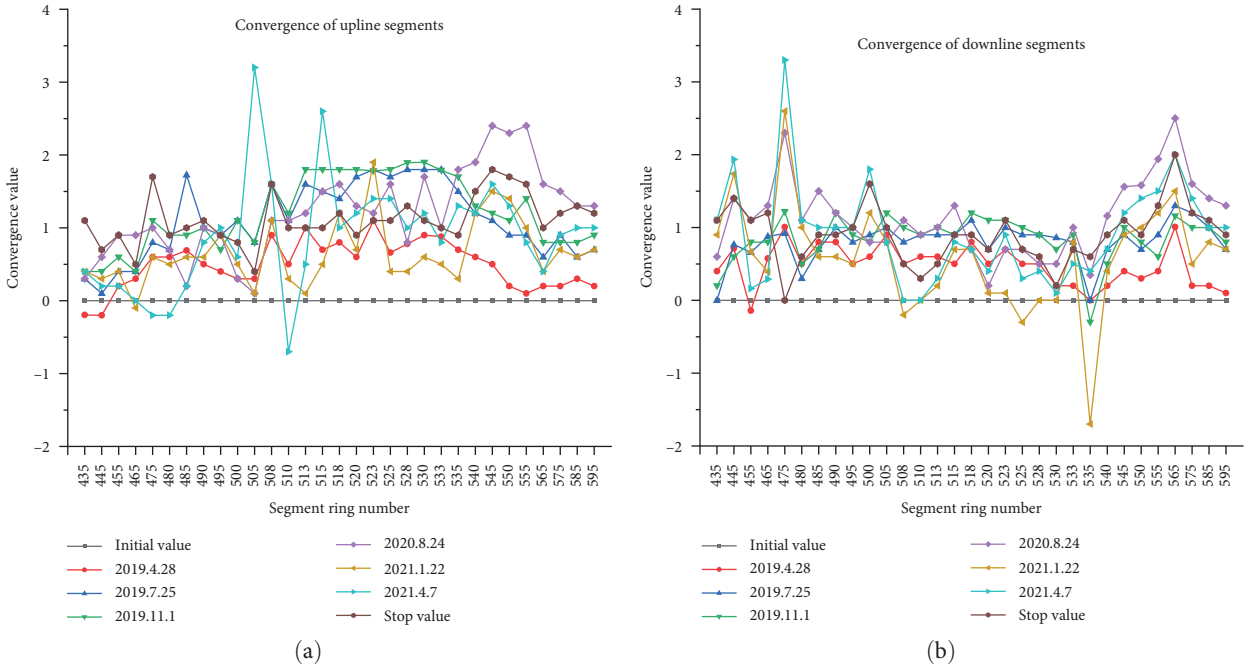

Figure 9: Segment convergence of existing tunnel under multiple disturbances.

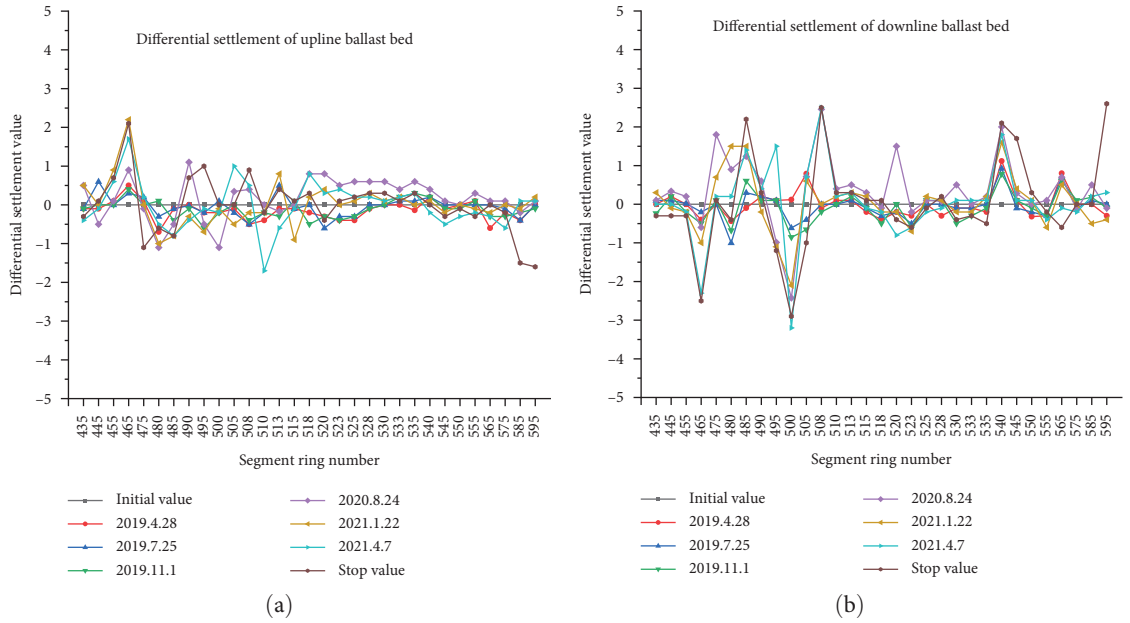

Figure 10: Differential settlement of ballast bed of existing tunnel under multiple disturbances.

In Figure 9(b), at the stage of soil reinforcement of the starting section, foundation pit excavation, and construction of the station main structure, the existing tunnel segments are vertically compressed and horizontally stretched. However, the convergence is slight, most of the values are below 1.0 mm, and some points reach 1.2 mm. The convergence value of 540–595 rings of segments slightly increases at the stage of right line shield tunneling across the existing line. The convergence values of 508–530 rings slightly decrease compared with that in the previous stage, and the other ranges are consistent with the results of convergence values after foundation pit excavation. During the foundation pit excavation of the entrance and exit of C, the existing tunnel is slightly affected, and the convergence value is the same as that in the previous stage. In general, the downline segment exhibits a state of vertical compression and transverse tension.

6.1.4. Differential Settlement of Ballast Bed. In Figure 10(a), at the stage of soil reinforcement of the starting section, foundation pit excavation, and construction of the station main

structure, the differential settlement of existing tunnel segments is not obvious and oscillates around the initial value. In the subsequent construction phase, only the 465- and 510-ring segments exhibited obvious segment torsion, and the maximum value appeared at the 465 ring, with a different settlement of 2.2 mm. The other segments were not significantly affected.

Similar to the upline, From inspection of Figure 10(b), the differential settlement of the existing tunnel segments is not obvious at the stage of soil reinforcement of the starting section, deep excavation, and construction of the main structure of the station. At the stage of right line shield tunneling over the existing line tunnel, the 465–508 rings in the influence area of the right line shield exhibit obvious differential settlement; some parts of the segment twist right, while others twist left. The 520 and 540 rings also exhibit significant differential settlement, with the maximum value appearing at the 508 ring and the differential settlement being 2.5 mm. Compared with the previous stage, the differential settlement of the tunnel ballast bed exhibits no significant changes at the stage of left line shield tunneling over the existing line, partly because of the reinforcement of the soil after synchronous grouting. Furthermore, this is because the disturbed segments have reached a state of equilibrium; thus, secondary shield tunneling can no longer significantly twist the segments. At the deep excavation stage of the entrance and exit of C, the differential settlement of the ballast bed of the existing tunnel is consistent with that in the previous stage, and there is no significant change.

6.2. Comparative Analysis of Data Changes at Typical Section Monitoring Points. Here, six typical sections are selected: the S513 and S528 sections intersecting the upline of Line 7 and Line 1; the S520 section corresponding to the middle part of the excavation face of the foundation pit; the X510 and X518 sections intersecting the downline of Line 7 and Line 1; the X523 section corresponding to the middle part of the excavation face of the foundation pit. By analyzing the monitoring data of typical sections at different construction stages, the deformation law of the existing tunnel is further investigated.

6.2.1. Vertical Displacement. As shown in Figure 11, during the soil reinforcement of the starting section period, each point has a slight settlement, but the upline is more obvious than the downline. During the excavation of the foundation pit, the points of the upline are consistent with those in the previous stage, whereas the downline has a significant settlement. At the construction stage of the main structure, the individual sections have a significant settlement, and generally, all points are still in the settlement trend. At the stage where the right shield crosses the existing line, S513 and X510 intersecting the new tunnel on the right line significantly uplift, with the upline uplift being higher than the downline uplift. However, sections S528 and X523 at the far end of the existing tunnel do not uplift, and even S528 still has a slight settlement. With the left line shield tunneling, there is a significant rise in all sections, especially S528, which intersects with the new tunnel on the left line. However, sections S513 and X510 at the far end of the existing

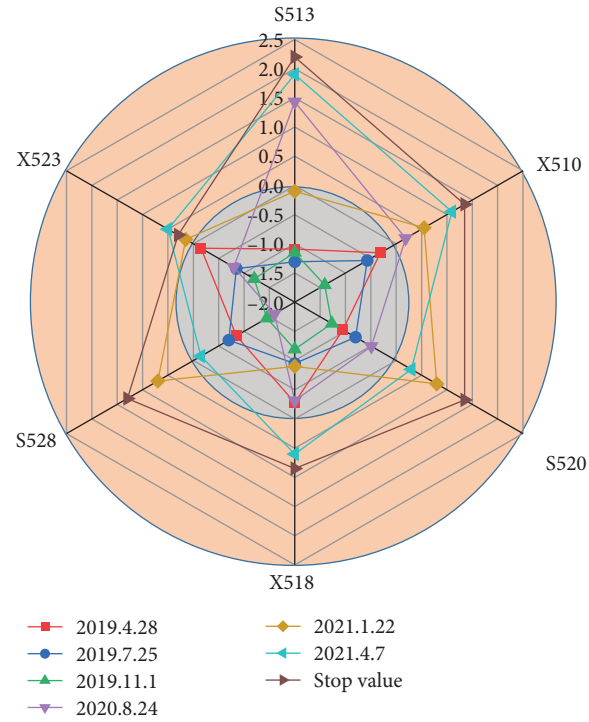

Figure 11: Vertical displacement at typical section.

tunnel settle and return to their original positions. At the subsequent construction stage, after several disturbances, each section still exhibits an uplift, and the value slightly increases toward the peak value.

6.2.2. Horizontal Displacement. According to the monitoring data of each typical section, during the soil reinforcement of the starting section period, each point exhibits a slight displacement toward the foundation pit. At the excavation stage, each point continues to move toward the foundation pit, and the value is between 1 and 2 mm. At the construction stage of the main structure, the horizontal displacement of each point is consistent with that in the previous stage. At the stage where the right shield crosses the existing line, horizontal displacement far away from the foundation pit appears at all points across the stage. The trend of each monitoring section on the upline is significantly higher than that on the downline, and the maximum value far away from the direction of the foundation pit is −3.8 mm. Regarding the left line, the trend of moving toward the foundation pit is slightly eased; however, in general, the trend of moving up the line is still more obvious than that of moving down the line. At the subsequent construction stage, all monitoring points are kept within the range from −1 to −2 mm, and the horizontal displacement values of the upper and lower sections are consistent, as shown in Figure 12.

6.2.3. Segment Convergence. As shown in Figure 13, soil reinforcement has little effect on segment convergence. The excavation results in the obvious convergence of each section segment, and the upline is significantly larger than the downline. During the construction phase of the main structure, the

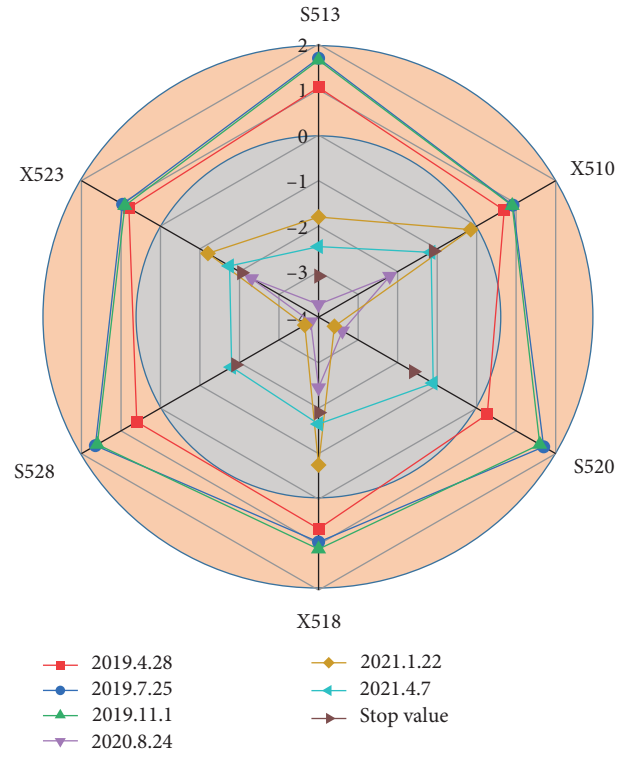

Figure 12: Horizontal displacement at typical section.

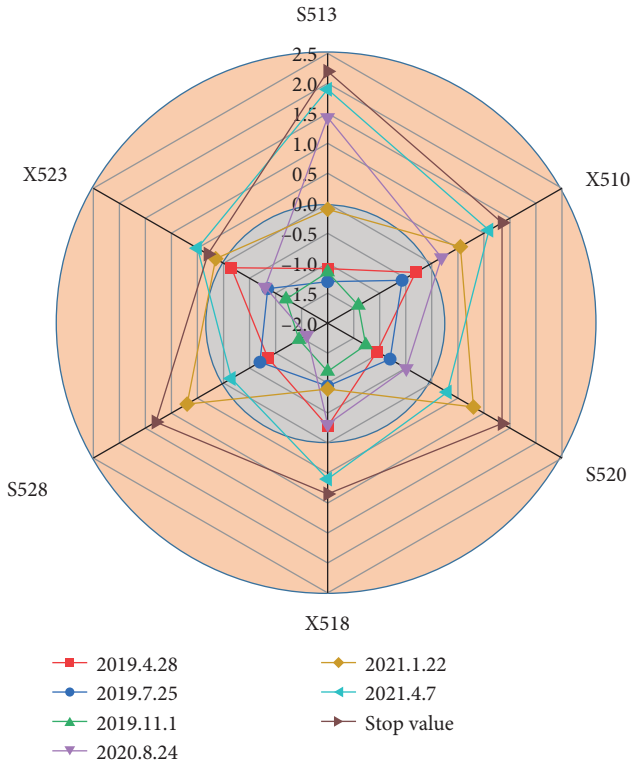

Figure 13: Segment convergence at typical section.

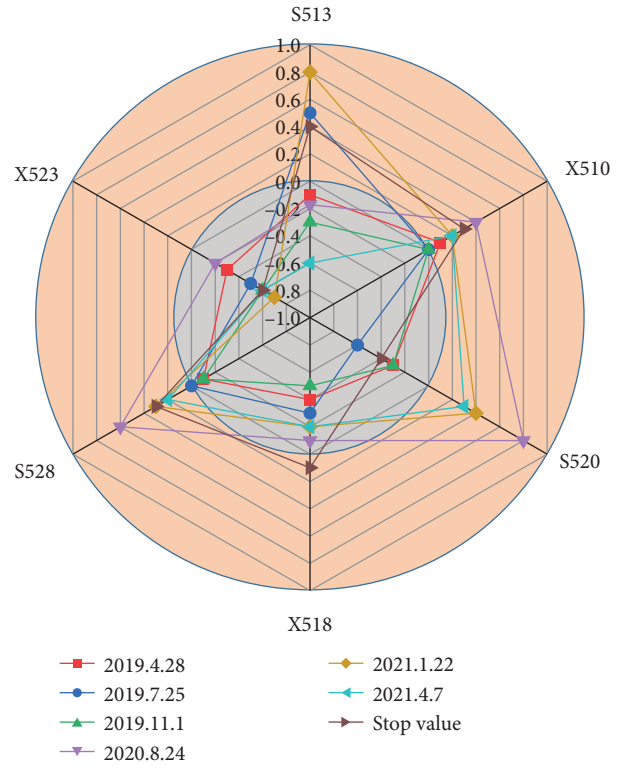

Figure 14: Differential settlement of ballast bed at typical section.

convergence of segments does not change significantly. At the stage where the right shield crosses the existing line, segment convergence decreases; however, overall, the upline is still higher than the downline. When the new tunnel of the left line crosses over the existing tunnel, the segment convergence trend is further reduced, bringing it close to the initial state, and there is no significant difference between the upper and lower lines. After the construction phase of the entrance and exit of C, the section close to entrance C again exhibits segment convergence with a maximum value of 1.1 mm.

6.2.4. Differential Settlement of Ballast Bed. Differential settlement of the ballast bed is manifested as torsion of the segment. According to the monitoring data in Figure 14, excavation of the foundation pit causes slight torsion in the positive direction of the S513 section. During the right line shield tunneling, segments far from the downline are twisted in a positive direction. When the left shield is driven, the monitoring section at the far end exhibits positive torsion. At the entrance and exit of C and the later stage, the torsion of the segment gradually returns to the initial state. In general, the influence of different construction stages on the differential settlement of the ballast bed is small.

6.2.5. Change Proportion of Typical Sections. After the existing tunnel is disturbed multiple times, the changing trends of segments in vertical displacement, horizontal displacement,

Table 3: Change proportion of the typical section of the upline.

Typical section segment number of the upline	Content of monitoring	Disturbance caused by excavation of foundation pit (mm)	Disturbance caused by new tunnel tunneling (mm)	Proportion of change (%)
S513	Vertical displacement	−1.3	−0.1	−92.3
	Horizontal displacement	1.7	−2.4	−241.2
	Segment convergence	1.6	0.1	−93.8
	Differential settlement of ballast bed	0.5	0.8	60.0
S520	Vertical displacement	−0.8	0.8	−200.0
	Horizontal displacement	1.7	−1.1	−164.7
	Segment convergence	1.7	0.7	−58.8
	Differential settlement of ballast bed	−0.6	0.4	−166.7
S528	Vertical displacement	−0.7	0.7	−200.0
	Horizontal displacement	1.7	−1.8	−205.9
	Segment convergence	1.8	0.4	−77.8
	Differential settlement of ballast bed	0.0	0.3	/

Table 4: Change proportion of the typical section of the downline.

Typical section segment ring of the downline	Content of monitoring	Disturbance caused by excavation of foundation pit/mm	Disturbance caused by new tunnel tunneling/mm	Proportion of change
X510	Vertical displacement	−0.6	0.6	−200.0%
	Horizontal displacement	0.9	−0.2	−122.2%
	Segment convergence	0.9	0.0	−100.0%
	Differential settlement of ballast bed	0.0	0.2	/
X518	Vertical displacement	−0.9	−0.9	0
	Horizontal displacement	0.9	−0.8	−188.9%
	Segment convergence	1.1	0.7	−36.4%
	Differential settlement of ballast bed	−0.3	−0.2	−33.3%
X523	Vertical displacement	−0.8	0.2	−125.0%
	Horizontal displacement	1.0	−1.2	−220.0%
	Segment convergence	1.0	0.1	−90.0%
	Differential settlement of ballast bed	−0.5	−0.7	40.0%

segment convergence, and differential settlement of the track bed are shown in Tables 3 and 4.

As shown in Tables 3 and 4, the vertical and horizontal displacements of the existing tunnel caused by foundation pit excavation and shield tunneling are opposite, and the influence is drastic, with the maximum range of change reaching 220%. Despite the obvious difference points of the downline ring X518, the vertical and horizontal displacements of the existing tunnel changed by 100%–200% in the opposite direction after the second disturbance. Pit excavation and shield tunneling also caused opposite changes in the convergence of existing tunnel segments; however, the influence is small, with a range of 36%–100%. Foundation pit excavation and shield tunneling have positive and negative effects on the differential settlement of the existing tunnel ballast bed; however, the overall effect is not significant.

7. Conclusions

(1) The vertical settlement of the existing tunnel is caused by deep excavation of the lateral top foundation pit. When the shield crosses over the existing tunnel for the first time, the underlying tunnel is uplifted because of soil unloading. When the shield machine disturbs the existing tunnel for the second time, the tunnel exhibits an uplift trend in some areas and a settling trend in others.

(2) The excavation of the foundation pit causes the horizontal displacement of the existing tunnel segments to move toward the foundation pit, and the crossing over of the shield causes the horizontal displacement of the existing tunnel toward the driving direction. The horizontal displacement of the existing tunnel

caused by shield tunneling is significantly larger than that caused by foundation pit excavation.

(3) The excavation of the foundation pit causes slight convergence of segments, and crossing over of the shield further aggravates the change in the convergence value, with some ranges increasing and some ranges decreasing. In general, excavation of the foundation pit and crossing over of the shield cause vertical compression and transverse stretching of the existing tunnel segments.

(4) The excavation of the foundation pit has little influence on segment torsion. The shield crossing over the existing line for the first time causes partial segment torsion of the existing line, and the direction of torsion cannot be determined. The second disturbance does not significantly affect segment torsion.

(5) In the foundation pit construction stage, the monitoring points on the typical section appear settled, and the settlement value of the points near the foundation pit is larger. When the new tunnel shield crosses over the existing tunnel, the existing tunnel segment corresponding to the overcrossing segment uplifts, while the distant segment settles. The excavation of the foundation pit causes the existing tunnel to move horizontally toward the foundation pit, and the tunneling causes the existing tunnel to move far away from the foundation pit. After several disturbances, the horizontal displacement of the existing tunnel away from the foundation pit is finally generated. Excavation of the foundation pit causes convergence of the existing tunnel segments. The convergence value of the point near the foundation pit is larger, and the overcrossing tunnel reduces the convergence of the segments. For differential settlement of the tunnel bed, regardless of the excavation of the foundation pit or overcrossing tunneling of the shield, the influence is slight.

(6) According to the analysis results of the monitoring data, the changing trend caused by multiple disturbances from the construction process to the existing tunnel is different. The deformation of the existing segment may dramatically change within a certain range; however, the displacement still fails to reach the alarm value. Therefore, during the excavation of the foundation pit, attention should be paid to the vertical settlement of the existing tunnel and the horizontal displacement toward the foundation pit. Monitoring of the uplift rate of the existing segment and the horizontal displacement rate away from the foundation pit should be strengthened during shield tunneling. The convergence of existing tunnel segments mainly occurs at the stage of foundation pit excavation and should be monitored. The excavation of the foundation pit and the overcrossing shield have little influence on the torsion of the existing segments, which cannot be taken as the key monitoring factor during construction.

Data Availability

The data used to support the findings of this study are included within the article.

Conflicts of Interest

The authors declare that they have no known competing financial interests or personal relationships that could have appeared to influence the work reported in this paper.

Acknowledgments

This work was financially supported by the National Science Foundation of China (nos. 51678062 and 51878060).

References

[1] Q. J. Meng, "Research on deformation and control of shield construction of four-line overlapping tunnels," *Chinese Journal of Underground Space and Engineering*, vol. 15, no. 3, pp. 911–919+926, 2019.

[2] J. Chai, S. Shen, W. Ding, H. Zhu, and J. Carter, "Numerical investigation of the failure of a building in Shanghai, China," *Computers and Geotechnics*, vol. 55, pp. 482–493, 2014.

[3] M. Y. Hu, J. T. Yang, L. D. Pan, K. S. Peng, and Y. K. Lu, "The effect of excavation unloading on the deformation of existing underlying shield tunnel," in *4th International Conference on Transportation Geotechnics*, 2022.

[4] R. Chen, F. Meng, Z. Li, Y. Ye, and J. Ye, "Investigation of response of metro tunnels due to adjacent large excavation and protective measures in soft soils," *Tunnelling and Underground Space Technology*, vol. 58, pp. 224–235, 2016.

[5] C.-T. Chang, C.-W. Sun, S. W. Duann, and R. N. Hwang, "Response of a Taipei Rapid Transit System (TRTS) tunnel to adjacent excavation," *Tunnelling and Underground Space Technology*, vol. 16, no. 3, pp. 151–158, 2001.

[6] C.-T. Chang, M.-J. Wang, C.-T. Chang, and C.-W. Sun, "Repair of displaced shield tunnel of the Taipei rapid transit system," *Tunnelling and Underground Space Technology*, vol. 16, no. 3, pp. 167–173, 2001.

[7] B. Nawel and M. Salah, "Numerical modeling of two parallel tunnels interaction using three-dimensional Finite Elements Method," *Geomechanics and Engineering*, vol. 9, no. 6, pp. 775–791, 2015.

[8] Z. Huang, D. Zhang, K. Pitilakis et al., "Resilience assessment of tunnels: framework and application for tunnels in alluvial deposits exposed to seismic hazard," *Soil Dynamics and Earthquake Engineering*, vol. 162, Article ID 107456, 2022.

[9] M. Son and E. J. Cording, "Estimation of building damage due to excavation-induced ground movements," *Journal of Geotechnical and Geoenvironmental Engineering*, vol. 131, no. 2, pp. 162–177, 2005.

[10] M. Vinoth and M. S. Aswathy, "Behaviour of existing tunnel due to adjacent deep excavation—a review," *International Journal of Geotechnical Engineering*, vol. 16, no. 9, pp. 1132–1151, 2022.

[11] M. G. Li, J. J. Chen, and J. H. Wang, "Arching effect on lateral pressure of confined granular material: numerical and theoretical analysis," *Granular Matter*, vol. 19, no. 2, pp. 3–11, 2017.

[12] H. Liu, P. Li, and J. Liu, "Numerical investigation of underlying tunnel heave during a new tunnel construction,"

Tunnelling and Underground Space Technology, vol. 26, no. 2, pp. 276–283, 2011.

[13] Z. G. Li, Y. Zeng, and G. B. Liu, "Numerical simulation of displacement transfer law in excavation of foundation pit adjacent to subway station," *Geotechnical Mechanics*, vol. 11, pp. 3104–3108, 2008.

[14] B. Liu, Z. W. Yua, Y. H. Han, Z. L. Wang, R. H. Zhang, and S. J. Wang, "Analytical solution for the response of an existing tunnel induced by abovecrossing shield tunneling," *Computers and Geotechnics*, vol. 124, pp. 1–15, 2020.

[15] Z. Zhang, M. Huang, and W. Wang, "Evaluation of deformation response for adjacent tunnels due to soil unloading in excavation engineering," *Tunnelling and Underground Space Technology*, vol. 38, pp. 244–253, 2013.

[16] H. Cheng, J. Chen, and G. Chen, "Analysis of ground surface settlement induced by a large EPB shield tunnelling: a case study in Beijing, China," *Environmental Earth Sciences*, vol. 78, no. 20, pp. 1–18, 2019.

[17] P. Li, Y. Lu, J. Lai, H. Liu, and K. Wang, "A comparative study of protective schemes for shield tunneling adjacent to pile groups," *Advances in Civil Engineering*, vol. 2020, Article ID 6640687, 12 pages, 2020.

[18] S. J. Ma, X. J. Li, Q. K. Wang, and Z. Ding, "Measured analysis of the influence of a deep foundation pit excavation on the adjacent existing shield tunnel," *Tunnel and Underground Engineering Disaster Prevention*, vol. 4, no. 1, pp. 86–94, 2022.

[19] P. Guo, F. Liu, G. Lei et al., "Predicting response of constructed tunnel to adjacent excavation with dewatering," *Geofluids*, vol. 2021, Article ID 5548817, 17 pages, 2021.

[20] X. Huang, H. Huang, and D. Zhang, "Centrifuge modelling of deep excavation over existing tunnels," *Proceedings of the Institution of Civil Engineers Geotechnical Engineering*, vol. 167, no. 1, pp. 3–18, 2014.

[21] C. W. W. Ng, J. Shi, D. Mašín, H. Sun, and G. H. Lei, "Influence of sand density and retaining wall stiffness on three-dimensional responses of tunnel to basement excavation," *Canadian Geotechnical Journal*, vol. 52, no. 11, pp. 1811–1829, 2015.

[22] C. W. W. Ng, H. S. Sun, G. H. Lei, J. W. Shi, and D. Mašín, "Ability of three different soil constitutive models to predict a tunnel's response to basement excavation," *Canadian Geotechnical Journal*, vol. 52, no. 11, pp. 1685–1698, 2015.

[23] H. Nie, K. Zhang, J. Lu, Q. Y. Bu, Y. Y. Zhou, and H. Gao, "Study on the influence of side excavation of foundation pit on shield tunnel," *Railway Survey*, vol. 45, no. 2, pp. 69–75, 2019.

[24] C. P. Gao, D. M. Zhang, and J. Y. Yan, "Risk analysis of the impact of unloading and reloading of adjacent engineering construction on the constructed shield tunnel," *Journal of Wuhan University (Engineering Science)*, vol. 49, no. 5, pp. 708–713+786, 2016.

[25] G. Wei, X. H. Zhang, X. B. Lin, and X. X. Hua, "Research on lateral force change of side shield tunnel caused by foundation pit excavation," *Geotechnical Mechanics*, vol. 41, no. 2, pp. 635–644+654, 2020.

[26] P. B. Peck, D. U. Deere, J. E. Moness, H. W. Parker, and B. Schmidt, "Some design considerations in the selection of underground support system," pp. 3–152, 1969, Report for Us Department of Transportation, Office of High Speed Ground Transportation, Contract.

[27] J.-I. Choi and S.-W. Lee, "Influence of existing tunnel on mechanical behavior of new tunnel," *KSCE Journal of Civil Engineering*, vol. 14, no. 5, pp. 773–783, 2010.

[28] C. He, "A study on the seismic behavior in the longitudinal direction of shield tunnels," Waseda University, Tokyo, The Dissertation for the Degree of Ph.D (in Japanese), 1999.

[29] A. Klar, T. E. Vorster, K. Soga, and R. J. Mair, "Elastoplastic solution for soil-pipetunnel interaction," *Journal of Geotechnical and Geoenvironmental Engineering*, vol. 133, no. 7, pp. 782–792, 2007.

[30] S. H. Kim, H. J. Burd, and G. W. E. Milligan, "Model testing of closely spaced tunnels in clay," *Geotechnique*, vol. 48, no. 3, pp. 375–388, 1998.

[31] T. Boonyarak and C. W. W. Ng, "Three-dimensional influence zone of new tunnel excavation crossing underneath existing tunnel," *Japanese Geotechnical Society Special Publication*, vol. 2, no. 42, pp. 1513–1518, 2016.

[32] L. Chen, H. W. Huang, and R. L. Wang, "Analysis of the influence of short-distance upper crossing on the settlement of the original tunnel," *Chinese Journal of Civil Engineering*, vol. 39, no. 6, pp. 83–87, 2006.

[33] C. Y. Gue, M. J. Wilcock, M. M. Alhaddad, M. Z. E. B. Elshafie, K. Soga, and R. J. Mair, "Monitoring the behaviour of an existing royal mail tunnel: London underground bond street station upgrade works," *Geotechnical Frontiers*, vol. 525, pp. 2017–2535, 2017.

[34] W. Guo, G. Wang, Y. Bao et al., "Detection and monitoring of tunneling-induced riverbed deformation using GPS and BeiDou: a case study," *Applied Science*, vol. 9, no. 13, Article ID 2759, 2019.

[35] M. Kavvadas, D. Litsas, I. Vazaios, and P. Fortsakis, "Development of a 3D finite element model for shield EPB tunnelling," *Tunnelling and Underground Space Technology*, vol. 65, pp. 22–34, 2017.

[36] A. Alsahly, J. Stascheit, and G. Meschke, "Advanced finite element modeling of excavation and advancement processes in mechanized tunneling," *Advances in Engineering Software*, vol. 100, pp. 198–214, 2016.

[37] N.-A. Do, D. Dias, P. Oreste, and I. Djeran-Maigre, "Three-dimensional numerical simulation for mechanized tunnelling in soft ground: the influence of the joint pattern," *Acta Geotechnica*, vol. 9, no. 4, pp. 673–694, 2014.

[38] K. L. Li, *Research on the Influence of New Tunnel Overpass Project on the Longitudinal Uplift Deformation of Existing Subway Tunnels*, Harbin Institute of Technology, 2017.

[39] C. S. Ding and X. F. Yang, "Analysis of the influence of shield tunnel overtravel on operating tunnels," *Construction Technology*, vol. 38, no. 1, pp. 48–50, 2009.

[40] Y. H. Yang, S. M. Liao, Y. Y. Fan, and J. Wu, "Deformation prediction and comparative analysis of shield tunneling up and down operating metro," *Chinese Journal of Rock Mechanics and Engineering*, vol. 30, no. S2, pp. 4072–4077, 2011.

[41] G. Zheng, Y. M. Du, Y. Diao, X. Deng, G. P. Zhu, and L. M. Zhang, "Influenced zones for deformation of existing tunnels adjacent to excavations," *Chinese Journal of Geotechnical Engineering*, vol. 38, no. 4, pp. 599–612, 2016.

[42] F. Y. Meng, R.-P. Chen, Y. Xu, K. Wu, H.-N. Wu, and Y. Liu, "Contributions to responses of existing tunnel subjected to nearby excavation: a review," *Tunnelling and Underground Space Technology*, vol. 119, Article ID 104195, 2022.

[43] R. Liang, T. Xia, Y. Hong, and F. Yu, "Effects of above-crossing tunnelling on the existing shield tunnels," *Tunnelling and Underground Space Technology*, vol. 58, pp. 159–176, 2016.